

# Refractive-Index Anisotropy and Optical Dispersion in Films of Deoxyribonucleic Acid

Anna Samoc,<sup>1</sup> Andrzej Miniewicz,<sup>1,2</sup> Marek Samoc,<sup>1</sup> James G. Grote<sup>3</sup>

<sup>1</sup>Laser Physics Centre, Research School of Physical Sciences and Engineering, Australian National University, Canberra, ACT 0200, Australia

<sup>2</sup>Institute of Physical and Theoretical Chemistry, Wrocław University of Technology, 50370 Wrocław, Poland

<sup>3</sup>Air Force Research Laboratory, Wright–Patterson Air Force Base, Ohio 45433

Received 12 May 2006; accepted 29 July 2006

DOI 10.1002/app.26082

Published online in Wiley InterScience (www.interscience.wiley.com).

**ABSTRACT:** We have determined the refractive indices in the directions parallel and perpendicular to the surface plane of films of deoxyribonucleic acid (DNA) and their wavelength dispersion. These parameters are fundamental for understanding the properties of waveguiding structures containing DNA-based photonic materials. The orientation of DNA molecules in films and their optical properties are sensitive to the film fabrication and environmental conditions influencing the structure. Prism coupling measurements show ambient-humidity-related changes in the refractive index, birefringence, and anisotropy of the alignment of the DNA molecules in the films studied. These films were 0.5–5  $\mu\text{m}$  thick, were prepared by both spin coating and casting from aqueous solutions containing 0.1–3 wt % DNA, and were measured in

ambient air with relative humidities of 37–58%. The optical properties of the films and the orientation of the DNA molecules are discussed with respect to the mechanism for the formation of the polymer liquid-crystalline phases during film deposition. The dispersion of the refractive indices in films of native DNA has been derived from interference fringes in absorption and reflection spectra in the wavelength range of 350–2700 nm through the fitting of the positions of the fringes with the Sellmeier dispersion formula in combination with the prism coupling data. © 2007 Wiley Periodicals, Inc. *J Appl Polym Sci* 105: 236–245, 2007

**Key words:** biopolymers; films; orientation; refractive index

## INTRODUCTION

This contribution, dedicated to the memory of the late Professor Kryszewski, discusses the properties of deoxyribonucleic acid (DNA) as a bio-organic polymer and its potential use for photonic applications. Five decades have passed since the discovery of the double-helix molecular structure of DNA<sup>1</sup> and its vital role in life processes and the long-term storage of genetic information. At that time, Kryszewski became a contributor to research in macromolecular science<sup>2</sup> and polymer physics,<sup>3</sup> augmenting our knowledge regarding the relationships between the molecular structure and macroscopic properties of

macromolecular substances. The work of Kryszewski and his coworkers resulted in many important observations and indications for further promising experiments and theoretical studies leading to applications of polymers, composites, and liquid-crystalline materials in photonics,<sup>4</sup> biosensing,<sup>5</sup> and biophysics.<sup>6</sup> His efforts in polarization spectroscopy studies of ordered optical chromophores, with stretched polyethylene as an orienting solvent, have made it possible to determine the transition dipole moment directions for electronic transitions in *trans*-stilbene and *trans*-azobenzene molecules.<sup>7</sup> On the basis of these results, it has been noted that these two molecules have very different geometries: *trans*-azobenzene has a nonplanar geometry, whereas *trans*-stilbene is more planar in the oriented polymer matrix. The phototransformation of the *trans* species in stretched polyethylene leads to a globular geometry of *cis*-azobenzene molecules with the phenyl rings twisted perpendicularly to the azo plane.<sup>8</sup> The process of the *trans*–*cis* photoisomerization of azobenzene molecules, intercalated into the base pairs of DNA, can be used in the photocontrolled formation and dissociation of a DNA triplex with ultraviolet (UV) and visible-light irradiation.<sup>9</sup> The triple-helix formation is considered one of the most promising methods for the sequence-specific recognition of DNA molecular

This article is dedicated to the memory of Professor Marian Kryszewski.

Correspondence to: A. Samoc (anna.samoc@anu.edu.au).

Contract grant sponsor: Asian Office of Aerospace Research and Development; contract grant number: AOARD-05-4010.

Contract grant sponsor: Australian Research Council Discovery; contract grant number: DP 0556942.

Contract grant sponsor: Materials and Manufacturing Directorate Air Force Office of Scientific Research.

*Journal of Applied Polymer Science*, Vol. 105, 236–245 (2007)  
© 2007 Wiley Periodicals, Inc.

memory (a memory that is based on DNA molecules and their molecular reactions).<sup>10</sup>

Recently, DNA has been considered a promising material for applications in photonics because of its exceptional chiral secondary structure and ability to act as a host for photochromic dyes.<sup>11</sup> A novel photonic biopolymer material has been fabricated from marine-based DNA by purification and then complexation with a cationic surfactant, cetyltrimethyl ammonium (CTMA) chloride,<sup>11–13</sup> or other cationic lipids.<sup>14,15</sup> In DNA–CTMA, the sodium ions are replaced with CTMA ions, which enable the solubility of the material in some organic solvents (e.g., 1-butanol). The DNA–CTMA biopolymer has been investigated for possible photonic applications in optical, electro-optical, optical memory, sensing, and optical amplifier systems.<sup>11–13,16–19</sup> Thin-film optical waveguides, prepared from a noncrosslinked DNA–CTMA biopolymer, have demonstrated low propagation losses. Losses of 1.25 and 1.79 dB/cm, at  $\lambda = 690$  nm, have been measured in noncrosslinked and crosslinked DNA–CTMA films, respectively.<sup>20</sup> The binding of fluorescent nonlinear optical dyes to DNA–CTMA, through intercalation, has led to the enhancement of the fluorescence quantum yield<sup>13</sup> and amplified spontaneous emissions, in which laser action is achieved without a laser cavity.<sup>21,22</sup> Recently, two-photon-excited, cavity-enhanced lasing was observed in a DNA–surfactant–chromophore complex gel system.<sup>23</sup>

It is important to identify what forms of DNA materials (native, sodium-based, or cation-replaced) are suitable for various applications in photonics. There is a lot of fundamental knowledge on the physical properties of nucleic acids and their structures and polymorphism.<sup>24–26</sup> However, not much is known about the methods for processing and their influence on optical and other physical properties of DNA, which are fundamental for the evaluation of the properties of waveguiding structures containing DNA-based photonic materials.

We are interested in the optical properties of DNA films fabricated from native DNA, sodium-ion-based DNA, and DNA–CTMA because of the unique double-helix structure. These biomolecules have the potential to induce the orientation of nonlinear optical chromophores used in photonic applications. Some chromophore dyes can be intercalated between the nucleic bases and lie roughly perpendicularly to the DNA helix axis. Other chromophore dyes can be oriented in the major and minor grooves of the DNA double helix and lie parallel to the helix axis.<sup>26,27</sup> The intercalation of the oriented nucleic acid with nonlinear optical dyes, two-photon absorption materials, fluorescence chromophores, and rare-earth compounds may bring new functionalities to DNA.

Thin films and fibers are the forms for materials that are most suitable for optical waveguiding applications. Therefore, we started our investigations of DNA with measurements of the optical properties of Na–DNA films. The refractive indices of DNA, published in refs. 12 and 13, reveal that self-assembled DNA thin films are anisotropic. There is also a small number of reports on refractive indices, birefringence, and optical dispersion in solid native DNA.<sup>28,29</sup> It appears that the anisotropy of the refractive index observed in a DNA film<sup>12,13</sup> is the opposite of that found in oriented DNA films and fiber bundles by others.<sup>29–32</sup>

We report here a range of results for the refractive indices in our DNA films as well as the refractive-index anisotropy and their dependence on the film preparation and storage conditions. Using a prism coupler, we measured the refractive indices in the orthogonal directions:  $n_{TE}$ , in the light polarization direction parallel to the surface of the thin film, and  $n_{TM}$ , in the light polarization direction perpendicular to the surface of the thin film (i.e., inside the film depth). The DNA films were prepared from solutions of a high-molecular-weight DNA biopolymer (ca. 12,000 base pairs). They were measured in ambient air with the relative humidity (RH) ranging from 37 to 58%. The refractive indices from prism coupler measurements were then used in the evaluation of the index dispersion, which was calculated from interference fringes in absorption and reflection spectra measured in UV, visible, and near-infrared wavelength ranges.

## EXPERIMENTAL

### Materials

Highly purified double-stranded Na–DNA was isolated from salmon milt and roe sacs (which are waste products of the Japanese fishing industry) and purified by an enzymatic isolation process at the Chitose Institute of Science and Technology, as described in ref. 18. The average molecular weight of the obtained DNA was  $8 \times 10^6$  Da (g/mol). This corresponds to  $12 \times 10^3$  nucleotide base pairs (the average molecular mass of the nucleotide base pair, 662 g/mol, was counted without water molecules bound to the DNA).

DNA aqueous solutions of pH 6–6.5 were prepared at room temperature, 21–22°C, through the dissolution of the fiberlike, white, solid material in deionized water. The concentration of DNA was in the range of 0.1–3 wt %. The solutions were made with a typical procedure in which the components were placed in a glass vial; the vial was closed with a poly(tetrafluoroethylene)-lined cap and placed on a rotating wheel for about 24 h for homogenization

by the solvent flow. Only the most concentrated solution (3 wt %) was homogenized with a magnetic stirring bar on a magnetic stage. The limit in the concentration, about 30 mg/mL for the high-molecular-weight salmon DNA, was due to the increasing viscosity of the solutions. Lowering the molecular weight of the DNA by, for example, ultrasonic processing helps reduce the viscosity.<sup>33</sup> However, we did not use this treatment here because of the possible effect of scission on the structure and optical properties of the films.

It is known that the properties of the nucleate ions in solutions and films are dependent on the pH and ionic strength of the solution, the types of counterions, the added electrolyte, the presence of other ions, the temperature, and even the previous treatment of the nucleic acid. In this project, we used aqueous, buffer-free, sodium-ion-based DNA solutions of a neutral pH, varying only the concentration of the solute and the method of film deposition. We characterized the solutions with electronic absorption spectra before the film deposition to learn about the purity and degree of denaturation of the solute, which was randomly selected from various batches of the supplied solid material. The spectra were measured with an ultraviolet-visible/near-infrared spectrophotometer (model 3101PC, Shimadzu, Shimadzu Scientific Instruments, Shimadzu Oceania, Rydalmere, New South Wales, Australia). They showed fair reproducibility of results and no sign of denaturation of the DNA. The average value of the specific absorption coefficient for the salmon DNA used, at the UV absorption maximum (258 nm), was found to be  $18.1 \pm 0.7 \text{ (mg/mL)}^{-1} \text{ cm}^{-1}$ , corresponding to a molar absorption coefficient of  $(6.0 \pm 0.2) \times 10^3 \text{ M}^{-1} \text{ cm}^{-1}$ . This value is about 10% lower than the literature data<sup>25</sup> for double-stranded DNA (from bacteria) in H<sub>2</sub>O solutions at a neutral pH, for which a molar absorption coefficient of  $6.6 \times 10^3 \text{ M}^{-1} \text{ cm}^{-1}$  was measured for the absorption peak at 260 nm. This corresponds to a specific absorption coefficient equal to  $20 \text{ (mg/mL)}^{-1} \text{ cm}^{-1} = 0.020 \text{ (}\mu\text{g/mL)}^{-1} \text{ cm}^{-1}$ . The lower molar absorption coefficient could be induced by a lower degree of purity of our material, a different base composition, or a hypochromic effect,<sup>25–27,34</sup> which gives a smaller molar absorption coefficient for better orientated nucleotide bases in the double-stranded DNA. The absorbance ratio  $A_{260}/A_{280}$  is used as a relative spectroscopic measure of the nucleic acid purity with respect to the protein content in a sample. A typical  $A_{260}/A_{280}$  value for pure, isolated DNA is 1.9.<sup>34</sup> A smaller ratio indicates increased contamination by proteins. The absorbance ratio  $A_{258}/A_{280}$ , which we evaluated in the measured spectra of solutions of randomly selected solid DNA fibers, had an average value of  $1.90 \pm 0.02$ . These estimations are in agreement with the given purity

percentage of the salmon DNA used (96%) with a protein content of 2%.<sup>18</sup>

### Film preparation

Thin films of salmon DNA were prepared through the casting and/or spinning of the DNA aqueous solutions on fused silica (Infrasil GE I24, Micro Materials and Research Consultancy Pty. Ltd., Melbourne, Australia) and indium tin oxide (ITO) coated (Thin Film Devices Inc., Anaheim, CA) glass substrates ( $24 \times 24 \times 1 \text{ mm}^3$ ). A Headway Research (Garland, TX) model 1-EC101D-R485 photoresist spinner was used for the film preparation. Films were dried in air at 21–22°C and about 40% RH on a laminar flow bench for about a day and stored in ambient air for several days. A list of the films prepared from the aqueous solutions of various Na-DNA concentrations is given in Table I. The various abbreviations of the films in Table I refer to the casting conditions only. A set of films (Table I) was additionally dried in a vacuum oven (Cole-Parmer, Extech Equipment, Boronia, Victoria, Australia) (model L-05053-12 vacuum oven with 1/4 DIN PID model L-89102-00 program controller) in a relatively low temperature range, 35–45°C, for 24 h. The chosen temperature range should allow drying of the films without denaturation of the material and a hyperchromic effect. The timescale in Table I was calculated against reference time zero when the set of films was removed from the vacuum oven (the minus sign denotes the earlier time, which includes 24 h of heating in the vacuum oven). The time between the film deposition and the end of the period of the vacuum drying was about 29 weeks for DNA-f1, about 6 days for DNA-f6, about 4 days for DNA-it6, about 5 days for DNA-f7, about 4 days for DNA-f8, and about 4 days for DNA-f9. After vacuum drying, the films were stored in ambient air in a laboratory-air-conditioned environment at a constant room temperature (21–22°C). However, the RH fluctuated a few percent within a day and from day to day. In general, the films were exposed to ambient air with the RH level in the range of 35–65%.

The RH was measured with a weather station equipped with a mechanical hygrometer, a thermometer, and a barometer. The RH data obtained with the analog hygrometer were comparable to the data measured with a TSI Q-Trak Plus IAQ Monitor (TSI Inc., Shoreview, MN) model 8554 electronic, digital thermohygrometer with CO (the RH accuracy was  $\pm 3\%$ , and the resolution was 0.1%).

The film absorption spectra were investigated in the wavelength range of 200–3200 nm with Shimadzu model UV-3101PC and Varian Cary (Varian Australia, Melbourne, Victoria, Australia) model 5000

TABLE I  
Refractive Indices of DNA Films Measured with a Prism Coupler in the Ambient Air at 22°C

Film <sup>a</sup>	Time since vacuum drying (weeks) <sup>b</sup>	RH (%)	$n_{TE}$ at 632.8 nm	$n_{TM}$ at 632.8 nm	$n_{TE} - n_{TM}$ at 632.8 nm	Thickness ( $\mu\text{m}$ )
DNA-f1 (Infrasil, casting and spinning at 600 rpm, and 3 wt %)	0.04	45	1.5577	1.5563	0.0014	2.1
	9.7	39	1.5480	1.5402	0.0078	1.5
	12.0	55	1.5371	1.5320	0.0051	1.7
	13.6	53	1.5293	1.5357	-0.0064	2.4
DNA-f6 (Infrasil, spinning at 200–700 rpm with many layers, and 0.15 wt %)	-0.27	40	1.5367	1.5627	-0.0260	0.50
	0.04	45	1.5483	1.5671	-0.0188	0.59
	9.7	38	1.5338	1.5330	0.0008	0.50
	12.6	58	1.5184	1.5454	-0.0270	0.53
DNA-it6 (ITO/glass, spinning at 120 rpm with many layers, and 0.15 wt %)	13.6	53	1.5309	1.5675	-0.0366	0.53
	-0.26	40	1.5352	1.5612	-0.0260	3.9
	0.04	45	1.5468	1.5633	-0.0165	4.0
	2.9	55	1.5263	1.5369	-0.0106	4.7
DNA-f7 (Infrasil, casting, and 0.20 wt %)	12.2	53	1.5130	1.5349	-0.0219	4.0
	13.6	53	1.5145	1.5409	-0.0264	4.6
	-0.30	41	1.5362	1.5607	-0.0245	2.1
	-0.30	39	1.5363	1.5608	-0.0245	2.2
DNA-f8 (Infrasil, casting, and 0.11 wt %)	0.02	45	1.5486	1.5654	-0.0168	2.1
	0.17	50	1.5446	1.5597	-0.0151	2.0
	3.0	50	1.5234	1.5420	-0.0186	2.5
	9.6	37	1.5424	1.5448	-0.0024	2.0
	12.2	53	1.5212	1.5403	-0.0191	2.6
	12.6	58	1.5153	1.5403	-0.0250	2.4
	13.6	54	1.5126	1.5417	-0.0291	2.7
	-0.29	37	1.5361	1.5668	-0.0307	2.2
DNA-f9 (Infrasil, spinning at 120–300 rpm with many layers, and 0.19 wt %)	-0.29	38	1.5367	1.5662	-0.0295	2.2
	0.02	45	1.5474	1.5732	-0.0258	1.8
	3.0	50	1.5225	1.5544	-0.0319	2.4
	9.7	45	1.5339	1.5628	-0.0289	1.8
	9.7	42	1.5353	1.5639	-0.0286	1.8
	9.7	40	1.5365	1.5648	-0.0283	1.8
	12.2	54	1.5062	1.5360	-0.0298	3.0
	12.6	56	1.5126	1.5431	-0.0305	3.0
DNA-f9 (Infrasil, spinning at 120–300 rpm with many layers, and 0.19 wt %)	13.6	53	1.5137	1.5442	-0.0305	2.9
	-0.28	39	1.5362	1.5616	-0.0254	4.8
	-0.27	40	1.5361	1.5622	-0.0261	4.4
	0.02	45	1.5505	1.5664	-0.0159	3.9
	3.0	50	1.5366	1.5420	-0.0054	3.8
	9.7	38	1.5418	1.5469	-0.0051	3.2
	9.7	38	1.5426	1.5458	-0.0032	3.8
	12.2	53	1.5309	1.5366	-0.0057	3.1
12.6	56	1.5282	1.5407	-0.0125	3.3	
13.6	54	1.5204	1.5462	-0.0258	2.5	

<sup>a</sup> The substrate, preparation method, and solution concentration are shown inside the parentheses.

<sup>b</sup> The films were dried in a vacuum oven at 35–45°C for 24 h and then stored in air at 22°C; the time is counted against time 0 when they were taken out of the oven. A minus sign indicates a time before the vacuum drying.

ultraviolet–visible/near-infrared scanning spectrophotometers. Prism coupler measurements enabling the determination of the refractive index and film thickness were taken before and after the vacuum drying, showing a response of a DNA film to the current humidity level. The refractive indices of the films at the same RH levels varied about 0.01. The thickness of the films was greater in the wet films; it decreased with drying and then increased at a higher humidity level. The thicknesses of the films were measured with a prism coupler and also with

alpha-step profiler. The thicknesses of the prepared films ranged from 0.5 to 4.8  $\mu\text{m}$  and for the various films were not uniform through the entire sample area but varied, as can be seen in Table I. The average thicknesses of the particular films were as follows:  $1.9 \pm 0.4 \mu\text{m}$  for DNA-f1,  $0.53 \pm 0.04 \mu\text{m}$  for DNA-f6,  $4.2 \pm 0.5 \mu\text{m}$  for DNA-it6,  $2.3 \pm 0.3 \mu\text{m}$  for DNA-f7,  $2.3 \pm 0.5 \mu\text{m}$  for DNA-f8, and  $3.7 \pm 0.7 \mu\text{m}$  for DNA-f9. The standard deviation indicates the magnitude of the variation of the film thickness at the spots measured in various regions of the films.



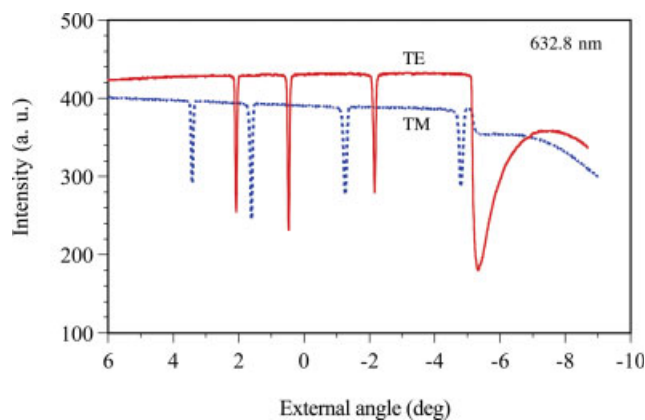


**Figure 1** Prism coupler reflectance curves measured in a film of salmon DNA (DNA-f7) on a silica substrate at RH  $\sim$  50%. The refractive indices ( $n_{TE} = 1.5445$  and  $n_{TM} = 1.5597$  at  $\lambda = 632.8$  nm) and the thickness ( $2.05 \mu\text{m}$ ) were computed from the modes obtained for the TE and TM polarization of a He-Ne laser light in the film. The film was dried *in vacuo* at 35–45°C for 24 h and then stored for 1 day in air before the prism coupler measurements. [Color figure can be viewed in the online issue, which is available at [www.interscience.wiley.com](http://www.interscience.wiley.com).]

### Prism coupler measurements

The refractive indices of the films were determined with the prism coupling technique using optical waveguiding in a film.<sup>35,36</sup> The indices were measured with a Metricon (Pennington, NJ) model 2010 prism coupler with a procedure in which the film was brought into contact with the base of a prism by means of a pneumatically operated coupling head. A laser beam, about 1–2 mm in diameter, with a wavelength of either 632.8 or 814 nm, was directed through the prism, striking the base of the prism at the coupling spot. The light beam was normally totally reflected at the prism base and was collected by a photodetector. However, at certain values of the incidence angle, light could tunnel across the air gap between the film and the prism at the coupling spot and enter into a waveguiding optical propagation mode in the film. This induced a sharp drop in the intensity of the light reflected from the base of the prism and created a dip in the reflectance curve measured by the detector (see Fig. 1). The index of the film was derived from the light propagation constant determined by the angular location of the modes and the index of the prism. The prism coupler measured the index of refraction of the film at the laser wavelength and could provide the film thickness if the film was sufficiently thick to support two or more optically guided modes. The instrument specifications were  $\pm 0.001$  for the index accuracy and  $\pm 0.0005$  for the index resolution. The thickness accuracy was  $\pm 0.5\%$ , and the thickness resolution was  $\pm 0.3\%$ .

Figure 1 shows examples of the reflectance curves obtained with the Metricon prism coupler in a

DNA film with transverse electric (TE) plane polarized light and transverse magnetic (TM) plane polarized light. For TE polarization, the electric field vector was parallel to the substrate; for TM polarization, the magnetic field vector was parallel to the substrate.

## RESULTS AND DISCUSSION

### Anisotropy of the refractive index

The refractive indices for the orthogonal TE and TM light polarizations are reported for six DNA films in Table I. The refractive-index data are presented against the time since the films were dried *in vacuo* at a slightly elevated temperature (35–45°C).

We were concerned about the identity of the material and the uniformity of the films at various coupling spots. We checked the reproducibility of the values of the refractive indices measured with light coupled into different spots on the films. The index values did not change substantially. For example, the difference between the refractive indices measured at two spots was only  $1 \times 10^{-4}$ , for both  $n_{TE}$  and  $n_{TM}$ , in film DNA-f7,  $(1-7) \times 10^{-4}$  in film DNA-f8, and  $(1-5) \times 10^{-4}$  in film DNA-f9 before vacuum drying. The refractive indices were found to be different at two different places by about  $9 \times 10^{-4}$  on film DNA-f9 when the film was measured at an RH of 38% after 10 weeks after drying. Therefore, we conclude that the optical properties did not vary substantially from spot to spot in these films. Also, the index fluctuation was within the instrument specification for the index accuracy measurements. However, the thickness of the films varied markedly between samples from spot to spot. The change ranged from a few percent in thinner films to about 20% in thicker films.

We observed that the refractive indices of DNA films were highly sensitive to the drying conditions and humidity of the environment during the measurements and storage (this effect is suppressed in DNA-CTMA films, as reported in detail elsewhere). Figure 2 shows the refractive-index data (plotted from Table I), which we measured in DNA films in ambient air with different RHs. The indices dropped markedly when the humidity in the laboratory environment reached a level of 55–60%.

An interesting observation can be made regarding the birefringence of the films. In most of the DNA films, the  $n_{TE}$  values (electric field vectors parallel to the surface of the film) were lower than the  $n_{TM}$  values (electric field vectors perpendicular to the surface of the film or along the film thickness). The birefringence ( $n_{TE} - n_{TM}$ ) was as high as  $-0.032$  in some films. Such a high value of the negative birefringence suggests a high degree of the orientation of DNA molecules in a film. This can be deduced

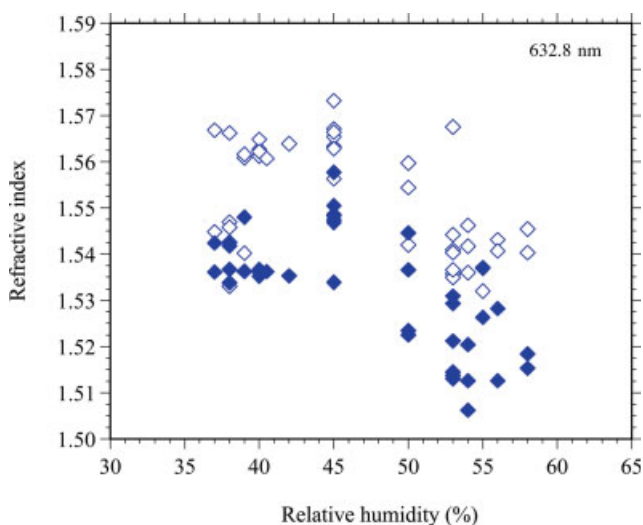


**Figure 2** Refractive indices ( $\blacklozenge$   $n_{TE}$  and  $\diamond$   $n_{TM}$ ) for six DNA films measured with a Metricon prism coupler at  $\lambda = 632.8$  nm and  $22^\circ\text{C}$  before and after vacuum drying for 24 h at  $35\text{--}45^\circ\text{C}$  and during 3 months of storage in ambient air with different RHs. [Color figure can be viewed in the online issue, which is available at [www.interscience.wiley.com](http://www.interscience.wiley.com).]

because the polarizability of the rigid-rod DNA molecule is larger in the direction perpendicular to the double helix axis than along it because of parallel stacking of the highly polarizable, anisotropic aromatic nucleotide bases. Therefore, the refractive index in the direction parallel to the nucleotide bases (i.e., across the DNA helix) is larger than that along the length of the molecular axis. The higher value of the refractive index observed for the E-field polarization direction perpendicular to the surface of the film suggests that the rigid-rod DNA molecules lie mostly parallel to the surface of the film.

The chain alignment in DNA films was induced spontaneously during film preparation in the process of drying the diluted solutions. The evaporation of the solvent causes the formation of a concentrated layer near the surface; the molecules can align along the air–liquid interface at the surface because of the interfacial effect.<sup>31,32</sup> In this mechanism, an evolution of a concentrated layer near the surface may lead to the transitional formation of a nematic-like, liquid-crystalline phase, resulting in an anisotropic, birefringent DNA film with good polymer chain alignment and orientation.

A careful inspection of the results in Table I reveals that some of our films were highly anisotropic, the molecules being aligned parallel to the film surface, some were nearly isotropic, and some even had an opposite anisotropy. The different structures of the films arise from the different preparation and environmental storage conditions. Figure 3 shows refractive indices for TE and TM polarization in two selected films (data from Table I). The film

DNA-f1, prepared by the spinning of a more concentrated solution (3 wt % DNA), was almost isotropic, whereas film DNA-f7, prepared via casting from a diluted DNA solution (0.20 wt % DNA) onto an identical substrate, was highly birefringent. The refractive properties of these films were also influenced by the humidity, but in a different way.

A small positive birefringence ( $n_{TE} > n_{TM}$ ) in a spin-deposited film of DNA-f1 (the data represented by squares in Fig. 3) indicated that the orientation of the DNA molecules was almost isotropic, with some orientation in the direction perpendicular to the surface of the film (the molecules adopted a spherulitic-like form). This weak birefringence changed its sign at an RH of 53%.

The other strongly negatively birefringent film, DNA-f7, had molecules highly aligned in the plane parallel to the surface ( $n_{TM} > n_{TE}$ ). The refractive indices were larger at a lower humidity, but the birefringence almost disappeared at an RH of 37%. The same happened to spin-deposited film DNA-f9. Spin-deposited film DNA-f6 showed an inversion in the sign of the birefringence at an RH of about 38%. These observations could be explained by the polymorphism of DNA and by the phase transitions observed in crystalline and semicrystalline fibers and films upon swelling and dehydration.<sup>26,37,38</sup>

It is possible that the mechanism of alignment of DNA chains may involve the formation of meso-

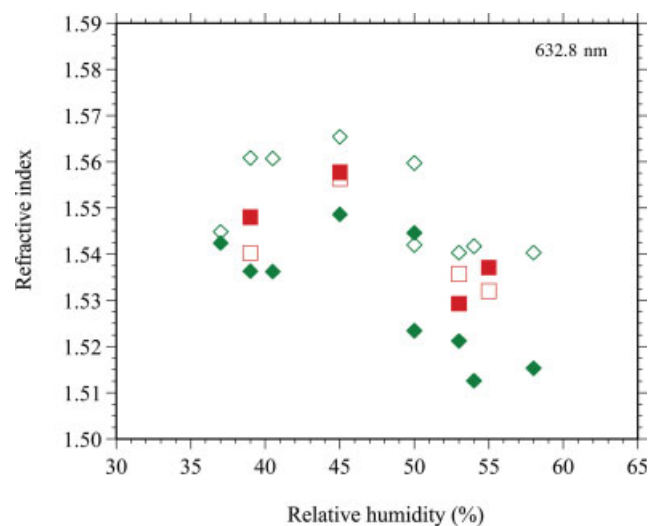


**Figure 3** Refractive indices at  $\lambda = 632.8$  nm of two selected DNA films measured with a prism coupler at  $22^\circ\text{C}$  in air with different RHs before and after vacuum drying (at  $35\text{--}45^\circ\text{C}$  for 24 h). The filled and open squares represent  $n_{TE}$  and  $n_{TM}$ , respectively, in spin-coated film DNA-f1 prepared from a 3 wt % DNA aqueous solution. The filled and open diamonds represent  $n_{TE}$  and  $n_{TM}$ , respectively, in film DNA-f7 prepared through the casting of a 0.20 wt % DNA aqueous solution on an Infrasil substrate. [Color figure can be viewed in the online issue, which is available at [www.interscience.wiley.com](http://www.interscience.wiley.com).]

scopic nematic, smectic, and cholesteric liquid-crystalline phases when the solvent evaporates during film formation and when the solute concentration reaches a critical value. Kagemoto et al.<sup>39</sup> showed that the phase states of DNA in concentrated solutions changed from an isotropic phase at a DNA concentration below 2 wt %, to an anisotropic phase in the concentration range of 3–5 wt % DNA, and to a liquid-crystalline phase at concentrations above 6 wt % DNA. The formation of lyotropic liquid-crystalline phases in more concentrated DNA solutions in the range of 100–300 mg/mL was also studied, for example, by Brandes and Kearns,<sup>30</sup> Strzelecka and coworkers,<sup>40,41</sup> Van Winkle and coworkers,<sup>42,43</sup> Rill et al.,<sup>44</sup> and Leforestier and Livolant.<sup>45</sup> A supra-molecular hexagonal columnar organization<sup>46</sup> and the formation of a hexatic phase between the cholesteric and crystalline phases have been reported for oriented DNA sheets.<sup>47</sup> The formation of ordered structures in films following the drying of 30–60 mg/mL solutions was reported in articles by Morii and coworkers.<sup>31,32</sup>

We inspected the morphology of the DNA films with cross-polarized, white-light microscopy under a low magnification. Preliminary observations revealed the presence of textures and patterns of stripes, distinctly ordered at the films' thicker edges, and occasionally colors, which might be related to the presence of the liquid-crystalline phases in the films.

Our DNA films showed a higher degree of birefringence and better chain alignment than those reported for films of higher molecular weight, 29,000-base-pair salmon DNA, for which the highest (negative) birefringence was 0.027.<sup>31</sup> Brandes and Kearns<sup>30</sup> observed a birefringence of  $0.02 \pm 0.005$  in a magnetically ordered liquid crystal at a concentration of 248 mg/mL calf thymus DNA. The difference in the liquid-crystalline behavior and optical properties can be explained by the different molecular weight of the DNA, the concentration of the solute, the presence of electrolyte ions, and the speed of film drying.

We see from our data that it is possible to obtain molecularly oriented DNA films with an isotropic or anisotropic chain orientation that is orthogonal to the planar orientation found in most of our films. A strong positive birefringence in a DNA film, reported by Wang et al.<sup>12</sup> and Zhang et al.,<sup>13</sup> for which  $n_{TE}$  was 1.534 and  $n_{TM}$  was 1.497, might have its origin in a film structure generated by the method of film processing and material preparation conditions; however, these parameters were not specified.

The values and anisotropy of the refractive indices found in our solution-cast films are in good agreement with the data obtained by Rupprecht et al.<sup>29</sup> in stretch-oriented, approximately 50- $\mu$ m-thick, fibril-like films of Na–DNA. The indices, measured at

$\lambda = 514.5$  nm, responded to the RH and were anisotropic. The refractive index perpendicular to the drawing axis was  $1.551 \pm 0.009$  at an RH of 45%. It was larger than the index in the direction parallel to the drawing axis,  $1.505 \pm 0.005$  at an RH of 45%.<sup>29</sup> These films were negatively birefringent, the birefringence was about 0.04–0.05 throughout most of the humidity range, and they were highly crystalline. The indices decreased with increasing water content, as in our films. Anomalous behavior was observed at RHs between 70 and 86%,<sup>29,37</sup> which was explained by the transition from the A phase to the B phase of DNA (the B phase occurs at a higher water content).

The optical constants of a DNA film *in vacuo* were measured by Inagaki.<sup>28</sup> The refractive index was 1.58 at  $\lambda = 620$  nm and 1.59 at  $\lambda = 496$  nm. Presumably, they were obtained in the film plane. They coincide poorly with the value of  $1.552 \pm 0.007$  measured at  $\lambda = 514.5$  nm *in vacuo* for the stretch-oriented film in the direction parallel to the drawing axis in ref. 29. Surprisingly, they are similar to the refractive-index data for the film *in vacuo* in the direction perpendicular to the drawing axis,  $1.583 \pm 0.006$ .<sup>29</sup>

These observations indicate that DNA is an exceptionally complex material that requires rigorous handling procedures and well-defined conditions of the film preparation methods to be able to predict the film properties. Of special interest, as possible tools to control the orientation and anisotropy of DNA films, are unique methods of preparation of oriented, lyotropic, liquid-crystalline films successfully developed by Kryszeński's group.<sup>4,48,49</sup>

### Dispersion of the refractive index

Inagaki et al.<sup>28</sup> measured the wavelength dependence of the refractive index in a DNA film *in vacuo* and at an RH of 92% in the range of 2–4 eV ( $\lambda = 620$ –310 nm). The change in the RH dramatically reduced the refractive index from 1.58 at an RH of 0% to about 1.43 at an RH of 92% at a photon energy of 2 eV.

The electronic spectra of DNA films show a prominent absorption peak at  $\lambda = 260$  nm, a valley at  $\lambda = 231$  nm in the UV range, and a relatively strong absorption peak in the IR range. This peak, with a maximum at about  $\lambda = 2990$  nm and a sideband at about  $\lambda = 3120$  nm, is caused by oscillation vibrations of the O–H and N–H bonds. The height of this peak depends on the RH and the content of water in the DNA films.

Absorption and reflection spectra of thin DNA films can often display fringes due to the interference of light being transmitted through the films with that reflected from the other interface. Figure 4 shows an example of fringes in the absorption spec-



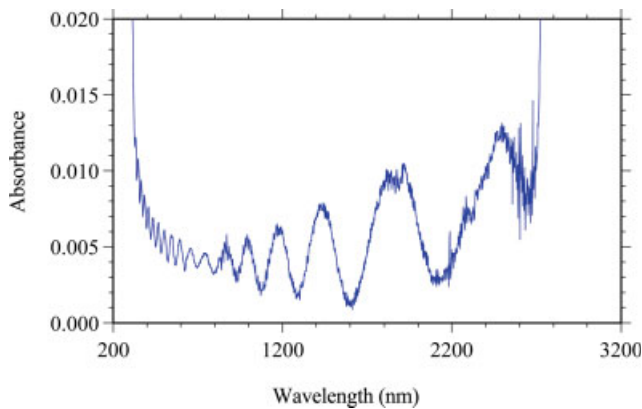


**Figure 4** Interference fringes in the absorption spectrum of film DNA-f7 on an Infrasil substrate measured in air (RH  $\sim$  45%) immediately after drying *in vacuo* (at 35–45°C for 24 h). The thickness of the film (2.07  $\mu\text{m}$ ), derived from the fitting of the fringe pattern with  $n_{TE} = 1.5486$  at  $\lambda = 632.8$  nm and  $n_{TE} = 1.5406$  at  $\lambda = 814$  nm, is in fair agreement with the thickness of the film (2.09  $\mu\text{m}$ ) measured with the prism coupler. [Color figure can be viewed in the online issue, which is available at [www.interscience.wiley.com](http://www.interscience.wiley.com).]

trum measured in a 2.07- $\mu\text{m}$ -thick film of DNA-f7 on a silica substrate.

We derived the dispersion of refractive indices in our DNA films from the interference fringes measured in the absorption and reflection spectra in a wide spectral range ( $\lambda = 200$ –3200 nm) at normal and oblique angles of incidence, respectively, employing a Cary 5000 spectrophotometer and a Shimadzu spectrophotometer. They provided data for a comparison with the results obtained with the prism coupling technique.

The transmission of light through a thin film depends on the values of the refractive index of the film [ $n(\lambda)$ ] and of both the substrate and the upper dielectric medium (air). A transmission spectrum contains fringes whose positions can be approximated with the following relation:  $I(\lambda) = I_0 \sin[2k(\lambda)d + \Delta\phi]$ , where  $I(\lambda)$  is the intensity of the transmitted light,  $I_0$  is the intensity of the incident light,  $k(\lambda) = 2\pi n(\lambda)/\lambda$  is the light propagation vector in the medium,  $\Delta\phi$  is a phase shift, and  $d$  is the thickness. The positions of these fringes can be used to obtain information on the thickness and refractive index of the film by, for example, the method of Swanepoel.<sup>50</sup> For light with normal incidence on a film of thickness  $d$ , the wavelengths of the transmission extremes are given by the well-known relation  $2nd = m\lambda$ , where  $m$  is the integer number counting maxima. In practice,  $n(\lambda)$  can be estimated for transparent films of thicknesses ranging from 0.5 to 5  $\mu\text{m}$ .

We analyzed the interference fringes in the absorption spectra to derive the thickness of the films, the refractive index, and its dispersion. We used a method similar to that of Swanepoel<sup>50</sup> in the ap-

proach, in which we made use of the knowledge of the refractive index of the film at a single wavelength and applied the Sellmeier dispersion equations for fitting the transmission fringes in a broad wavelength range. We chose to approximate the index dispersion [ $n(\lambda)$ ] by a Sellmeier-type formula:

$$n(\lambda) = \left( A + \frac{B}{1 - \frac{C}{\lambda^2}} \right)^{0.5} \quad (1)$$

which requires knowledge of dispersion parameters  $A$ ,  $B$ , and  $C$ .

We performed many measurements of absorption and reflectance spectra of the pure DNA films listed in Table I. The fringe patterns were fitted with the Mathcad 2000 program (Mathsoft, Cambridge, MA); we adjusted the parameters in the Sellmeier formula to achieve the same number and position of all the measured maxima and minima in the entire spectral region.

The refractive indices of the DNA depended to a marked degree on factors such as the RH, as shown in Table I. From the measurements, an average index dispersion formula was derived, that is, a Sellmeier-type equation, which could be used in the case of our DNA films. For salmon DNA films prepared from deionized water solutions, we found this relation:

$$n(\lambda) = \left( 1.028 + \frac{1.286}{1 - \frac{14000}{\lambda^2}} \right)^{0.5} \quad (2)$$

where  $\lambda$  is measured in nanometers. In the case of DNA films for which the refractive index was very sensitive to the content of water, the first parameter ( $A$ ) of the equation had to be varied to some extent to obtain a good fit to the measured thickness and refractive index for films under different humidity conditions, whereas the  $B$  and  $C$  parameters did not require such variation. Equation (2) gives  $n_{TE} = 1.5364$  at  $\lambda = 632.8$  nm and  $n_{TE} = 1.5303$  at  $\lambda = 814$  nm as possible values of the refractive index at, for example, RH  $\sim$  50%.

The fitting of the fringes in the spectrum in Figure 4 for DNA film DNA-f7, 2.07  $\mu\text{m}$  thick, measured at RH  $\sim$  45%, gave the dispersion parameters  $A = 1.0655$ ,  $B = 1.2858$ , and  $C = 14000$ . The absence of in-plane anisotropy was detected for the refractive index of the studied DNA films, at least within the accuracy of the absorption and reflectance methods. The prism coupler values,  $n_{TE} = 1.5486$  at  $\lambda = 632.8$  nm and  $n_{TE} = 1.5406$  at  $\lambda = 814$  nm, were obtained for this film at RH  $\sim$  45%, following the measurement of the spectrum in the same film area. For the measurements of the reflection spectra, we used a variable-angle specular reflectance accessory designed



for the Cary 5000 spectrophotometer, allowing for reflectance measurements at angles between 20 and 70°. However, we will report this in detail elsewhere. The use of the absorption interference fringe technique can be advantageous for studies of the uniformity of the optical properties of DNA-based films.

## CONCLUSIONS

Our films of double-stranded DNA, derived from salmon milt and roe sacs, demonstrated interesting linear optical properties. We prepared a series of films, using both spin-coated and cast aqueous solutions, in a range of concentrations of the DNA solute (0.1–3 wt %). The solutions were characterized with absorption spectra. The films were measured with a prism coupling technique to obtain refractive indices for TE and TM light polarization. The absorption and reflection spectra showed interference fringes, which could be used to derive information on the refractive-index dispersion.

We observed that the values of the refractive indices and birefringence in the DNA films varied considerably, depending on the film fabrication method, solution concentration, drying conditions, and RH of the environment.

The refractive indices of the DNA films decreased with increasing humidity in ambient air. Prism coupler measurements showed various degrees of optical anisotropy for the films.

A high negative birefringence, about  $-0.03$  at RH  $\sim 55\%$ , in the solution-cast films, indicated that the DNA molecules were highly aligned in a plane parallel to the film surface. However, this alignment changed with the humidity. The birefringence almost disappeared at RH  $\sim 37\%$ . This might suggest a transition to a different phase, a change in the orientation, or a change in the shape of the molecules.

An almost isotropic DNA polymer film made by spin deposition of a more concentrated solution (3 wt % DNA) had a slightly positive birefringence. This suggests that the molecules were randomly orientated. We saw a fluctuation in the birefringence in this film at RH  $\sim 53\text{--}55\%$ , indicating a change in its molecular organization.

We are keen to rationalize the fluctuations in the optical data with respect to the polymorphism and liquid-crystalline forms of DNA. The polymer may form mesoscopic liquid-crystalline phases during the process of densification of a solution by solvent evaporation and the formation of a solid film. The difference in the optical anisotropy of the cast and spin-coated films might have its origin in the different speeds of solvent evaporation and the concentration-dependent freedom of the alignment of the DNA molecules. The humidity-dependent fluctua-

tions of the birefringence indicate a change in the local structure and organization of the DNA molecules in the moisture-swollen solid films.

The authors acknowledge the pioneering efforts of Naoya Ogata of the Chitose Institute of Science and Technology for providing the source of deoxyribonucleic acid used in their research.

## References

1. Watson, J. D.; Crick, F. H. *Nature* 1953, 171, 737.
2. Kryszewski, M. *Roczniki Chem* 1952, 26, 350.
3. Kryszewski, M. *Roczniki Chem* 1955, 29, 1041.
4. Ulanski, J.; Wojciechowski, P.; Kryszewski, M. *Mol Cryst Liq Cryst Sect B* 1995, 9, 203.
5. Kryszewski, M. *Photonics Sci News* 1998, 3, 28.
6. Kryszewski, M. *Acta Phys Pol A* 2004, 105, 389.
7. Uznanski, P.; Kryszewski, M.; Thulstrup, E. W. *Spectrochim Acta A* 1990, 46, 23.
8. Uznanski, P.; Kryszewski, M.; Thulstrup, E. W. *Eur Polym J* 1991, 27, 41.
9. Liang, X.; Asanuma, H.; Komiyama, M. *J Am Chem Soc* 2002, 124, 1877.
10. Takinoue, M.; Sauyama, A. *Chem-Biol Inf J* 2004, 4, 93.
11. Watanuki, A.; Yoshida, J.; Kobayashi, S.; Ikeda, H.; Ogata, N. *Proc SPIE-Int Soc Opt Eng* 2005, 5724, 234.
12. Wang, L.; Yoshida, J.; Ogata, N.; Sasaki, S.; Kajiyama, T. *Chem Mater* 2001, 13, 1273.
13. Zhang, G.; Wang, L.; Yoshida, J.; Ogata, N. *Proc SPIE-Int Soc Opt Eng* 2001, 4580, 337.
14. Tanaka, K.; Okahata, Y. *J Am Chem Soc* 1996, 118, 10679.
15. Yamaoka, K.; Kagami, Y.; Wada, M.; Watanuki, A.; Yoshida, J.; Ikeda, H.; Ogata, N. *Proc SPIE-Int Soc Opt Eng* 2005, 5624, 193.
16. Grote, J. G.; Ogata, N.; Diggs, D. E.; Hopkins, F. K. *Proc SPIE-Int Soc Opt Eng* 2003, 4991, 621.
17. Hagen, J. A.; Grote, J. G.; Ogata, N.; Zetts, J. S.; Nelson, R. L.; Diggs, D. E.; Hopkins, F. K.; Yaney, P. P.; Dalton, L. R.; Clarson, S. J. *Proc SPIE-Int Soc Opt Eng* 2004, 5351, 77.
18. Grote, J. G.; Diggs, D. E.; Nelson, R. L.; Zetts, J. S.; Hopkins, F. K.; Ogata, N.; Hagen, J. A.; Heckman, E.; Yaney, P. P.; Stone, M. O.; Dalton, L. R. *Mol Cryst Liq Cryst* 2005, 426, 3.
19. Yaney, P. P.; Heckman, E. M.; Diggs, D. E.; Hopkins, F. K.; Grote, J. G. *Proc SPIE-Int Soc Opt Eng* 2005, 5724, 224.
20. Heckman, E. M.; Yaney, P. P.; Grote, J. G.; Hopkins, F. K. *Proc SPIE-Int Soc Opt Eng* 2005, 5934, 52.
21. Kawabe, Y.; Wang, L.; Horinouchi, S.; Ogata, N. *Adv Mater* 2000, 12, 1281.
22. Kawabe, Y.; Wang, L.; Nakamura, T.; Ogata, N. *Appl Phys Lett* 2002, 81, 1372.
23. He, G. S.; Zheng, Q.; Prasad, P. N.; Grote, J. G.; Hopkins, F. K. *Opt Lett* 2006, 31, 359.
24. Jordan, D. O. In *The Nucleic Acids Chemistry and Biology*; Chargaff, E.; Davidson, J. N., Eds.; Academic: New York, 1955; p 447.
25. Freifelder, D. *Physical Biochemistry*; Freeman: San Francisco, 1982.
26. Saenger, W. *Principles of Nucleic Acid Structure*; Springer-Verlag: New York, 1984.
27. Beaven, G. H.; Holiday, E. R.; Johnson, E. A. In *The Nucleic Acids Chemistry and Biology*; Chargaff, E.; Davidson, J. N., Eds.; Academic: New York, 1955; p 493.
28. Inagaki, T.; Hamm, R. N.; Arakawa, E. T.; Painter, L. R. *J Chem Phys* 1974, 61, 4246.
29. Weidlich, T.; Lindsay, S. M.; Rupprecht, A. *Biopolymers* 1987, 26, 439.

30. Brandes, R.; Kearns, D. R. *Biochemistry* 1986, 25, 5890.
31. Morii, N.; Kido, G.; Suzuki, H.; Nimori, S.; Morii, H. *Biomacromolecules* 2004, 5, 2297.
32. Morii, N.; Kido, G.; Suzuki, H.; Morii, H. *Biopolymers* 2005, 77, 163.
33. Heckman, E. M.; Hagen, J. A.; Yaney, P. P.; Grote, J. G.; Hopkins, F. K. *Appl Phys Lett* 2005, 87, 211115.
34. Boyer, R. F. *Modern Experimental Biochemistry*; Addison-Wesley: Reading, MA, 1986.
35. Ulrich, R.; Torge, R. *Appl Opt* 1973, 12, 2901.
36. Tien, P. K. *Rev Mod Phys* 1977, 49, 361.
37. Lindsay, S. M.; Lee, S. A.; Powell, J. W.; Weidlich, T.; Demarco, C.; Lewen, G. D.; Tao, N. J.; Rupprecht, A. *Biopolymers* 1988, 27, 1015.
38. Lewen, G.; Lindsay, S. M.; Tao, N. J.; Weidlich, T.; Graham, R. J.; Rupprecht, A. *Biopolymers* 1986, 25, 765.
39. Kagemoto, A.; Nakazaki, M.; Kimura, S.; Momohara, Y.; Ueno, K.-I.; Baba, Y. *Thermochim Acta* 1996, 284, 309.
40. Strzelecka, T. E.; Davidson, M. W.; Rill, R. L. *Nature* 1988, 331, 457.
41. Strzelecka, T. E.; Rill, R. L. *Biopolymers* 1990, 30, 57.
42. Van Winkle, D. H.; Davidson, M. W.; Chen, W. X.; Rill, R. L. *Macromolecules* 1990, 23, 4140.
43. Van Winkle, D. H.; Davidson, M. W.; Rill, R. L. *J Chem Phys* 1992, 97, 5641.
44. Rill, R. L.; Strzelecka, T. E.; Davidson, M. W.; Van Winkle, D. H. *Phys A* 1991, 176, 87.
45. Leforestier, A.; Livolant, F. *Biophys J* 1993, 65, 56.
46. Livolant, F. *J Mol Biol* 1991, 218, 165.
47. Strey, H. H.; Wang, J.; Podgornik, R.; Rupprecht, A.; Yu, L.; Parsegian, V. A.; Sirota, E. B. *Phys Rev Lett* 2000, 84, 3105.
48. Wojciechowski, P.; Okrasa, L.; Ulanski, J.; Kryszewski, M. *Adv Mater Opt Electron* 1996, 6, 383.
49. Kryszewski, M. *Nonlinear Opt Quant Opt* 2004, 31, 45.
50. Swanepoel, R. *J Opt Soc Am* 1985, 2, 1339.